ACADEMIC PRESS

Available online at www.sciencedirect.com

SCIENCE DIRECT®

Journal of Magnetic Resonance 162 (2003) 320–327

JMR Journal of Magnetic Resonance

www.elsevier.com/locate/jmr

Diffusion–relaxation correlation in simple pore structures

P.T. Callaghan,* S. Godefroy, and B.N. Ryland

MacDiarmid Institute for Advanced Materials and Nanotechnology, School of Chemical and Physical Sciences, Victoria University of Wellington, Wellington, New Zealand

Received 8 October 2002; revised 10 February 2003

Abstract

The effects of independent encoding for relaxation and for diffusion using separate time and gradient dimensions are calculated for spins diffusing in plane parallel and spherical pores with relaxing walls. Two-dimensional inverse Laplace transformation is used to obtain computed (D, T_2) maps for both geometries, in the regime in which the dimensionless diffusion coefficient is less than unity and the dimensionless relaxation parameter of order unity or greater. It is shown that there exist two distinct branches on the (D, T_2) maps, one with diffusion and relaxation strongly correlated and one in which the diffusion coefficients vary widely independently of relaxation.

Keywords: Diffusion; Relaxation; Two-dimensional; Laplace; Porous media

1. Introduction

The problem of restricted diffusion in simple pore structures forms a paradigm for many practical applications of NMR in porous media, for example in oil well logging, separation science, reactor technology, microfiltration, plant physiology, and biomedicine. The original platform for NMR analysis was provided in a classic paper by Brownstein and Tarr [1] in which they predicted multi-exponential relaxation for spins carried by molecules undergoing restricted diffusion in a pore with relaxing walls. In particular they solved this relaxation–diffusion problem for planar, cylindrical, and spherical pores using eigen-mode expansions and obtained exact analytic expressions for the amplitudes and time constants of the multi-exponential relaxation. The dimensionless parameter which defines the problem is the ratio Ma/D_0, where M is the wall relaxivity, a characterizes the pore dimension, and D_0 is the (unrestricted) self-diffusion coefficient of the fluid within the pore. Brownstein and Tarr showed that the dominant term in the spin relaxation was associated with a relaxation time which depends on the pore dimension as a/M for Ma/D_0 small and a^2/D_0 for Ma/D_0 large. This behavior forms the basis of pore size analysis through NMR relaxivity measurement. The primary mathematical tool for deriving a distribution of relaxation times (and hence pore sizes) from multi-exponential signal decay is inverse Laplace transformation [2–4].

During the last decade the effects of diffusion restriction in porous media have been studied using another NMR method, the Pulsed Gradient Spin Echo technique [5–10] in which the echo attenuation is measured as a function of gradient wavevector $\mathbf{q}$ and the diffusive observation time Δ. At values of Δ sufficiently large that many spin-bearing molecules reach the walls $(D_0\Delta/a^2 > 1)$ this "signal", $E(\mathbf{q}, \Delta)$, exhibits coherence phenomena in the $\mathbf{q}$-domain reminiscent of diffraction [10–16]. The problem is amenable to exact analytic solution in the case of planar, cylindrical, and spherical pores and expressions have been published [17] which also take into account wall relaxation during the diffusion encoding period.

In principle the relaxation response and the $\mathbf{q}$-vector response of the system are separable using an experiment in which relaxation and diffusive effects are encoded in two independent dimensions on the same NMR magnetization using classical two-dimensional NMR methodology. The experiment consists in applying a Carr–Purcell–Meiboom–Gill pulse train (or an inversion recovery period) in which the time over which

* Corresponding author. Fax: +646-350-5164.
E-mail address: p.callaghan@massey.ac.nz (P.T. Callaghan).

1090-7807/03/$ - see front matter
doi:10.1016/S1090-7807(03)00056-9

transverse (or longitudinal) relaxation occurs is varied, followed (or preceded) immediately by a PGSE pulse sequence in which the **q**-value is independently changed. In the relaxation domain the appropriate data analysis is inverse Laplace transformation. In the **q**-domain, either Fourier transformation with respect to **q** can be used, in which case the averaged propagator for displacement is returned, or inverse Laplace transformation with respect to q^2 can be used, in which case a distribution of effective diffusion coefficients is returned. The former approach was taken by Britton et al. [18] who obtained a relaxation time-propagator map for water flowing in a porous bead pack, while the latter was taken by Lee et al. [19] and by Hürlimann and Venkataramanan [20] who calculated relaxation–diffusion maps for water in a porous rock sample.

The double Laplace inversion technique used in the Hürlimann and Venkataramanan experiment was developed by Venkataramanan et al. [21] and first demonstrated by Song et al. [22]. Because of the ill-posed nature of the mathematical problem associated with 1-D Laplace inversion, the matter of 2-D inversion is especially delicate. The solution by Venkataramanan et. al. [21] is elegant. They reduced the size of the 2-D matrices associated with the data sets and the inversion kernel using Singular Value Decomposition, and then transformed the 2-D matrices associated with the input and output data sets to 1-D vectors by consecutive ordering of the matrix rows or columns. By this means they transformed the problem back to a 1-D Non-Negative Least Squares (NNLS) format, with large but manageable vector space dimensions. This important development opens the way for a wide range of new two-dimensional NMR experiments in which independent multi-exponential processes are correlated. The present paper attempts to assist that process by returning attention to the simplest of all possible problems. In particular we seek to demonstrate here just how relaxation–diffusion correlation is manifest in the case of planar and spherical pores with relaxing walls.

Here we present analytic expressions for the two-dimensional echo amplitudes and show the relaxation–diffusion maps which result over a range of values of the key dimensionless parameters, Ma/D_0 and $D_0\Delta/a^2$. This work is in the spirit of earlier papers [16,17] in which the one-dimensional q-response was outlined. It will be apparent in the analysis presented here that the relaxation–diffusion behavior, in even the simplest of pore geometries, is exceedingly complex. That complexity serves as a cautionary reminder that we need a sound platform from which to interpret behaviors exhibited in more general porous media. But the complexity is also a source of potentially rich information and we shall attempt to identify some insights made possible by the separation of relaxation and diffusion along orthogonal dimensions. As a precursor to that, we note that several authors have previously investigated the combined effect of PGSE and relaxation encoding [18,23–25]. However, to our knowledge, the application of 2-D Laplace inversion techniques to the study of simple pore geometries is novel. As we shall show, this 2-D approach is instructive in separating the Brownstein–Tarr modes associated with wall relaxation.

Taking the simplest possible (and somewhat naïve) perspective we point out the following interaction between the independent relaxation and PGSE encodings. Wall relaxation preferentially attenuates signals from spins near the walls whose relaxation is enhanced, thus overemphasizing the spins at the interior for the PGSE experiment. By contrast PGSE preferentially attenuates signals from interior spins, whose diffusion is not impeded by the wall, thus overemphasizing the spins near the walls in the relaxation experiment. This picture is simplistic since it assumes a subdivision of populations by volume, a process which is only meaningful for large values of the relaxation parameter Ma/D_0 and small values of the diffusion parameter, $D_0\Delta/a^2$. Nonetheless, there is another sense in which we may wish to restrict our attention to small values of the diffusion parameter. As pointed out above, for $D_0\Delta/a^2$ of order unity or larger, diffraction effects become apparent in the PGSE **q**-space dependence, thus rendering inverse Laplace transformation meaningless. Indeed we will only observe an echo attenuation behavior describable by a superposition of exponential decays where $D_0\Delta/a^2$ is small compared with unity. This condition can always be achieved experimentally by making the diffusion encoding time Δ sufficiently short.

2. Theory

The basic NMR pulse sequence used to encode for both spin relaxation and diffusion is shown in Fig. 1. We choose, for convenience, to assume a prior encoding for relaxation. The time order is not significant. We further allow for relaxation during the PGSE encoding time, Δ. The theoretical procedure is well described in an earlier paper [17]. The first RF pulse generates an initial transverse magnetization density, $\rho(\mathbf{r},0)$, which is assumed uniform through the pore. The subsequent behavior of that magnetization, $\rho(\mathbf{r},t)$, is governed by the relaxation at the pore boundaries, by phase changes, $\exp(\mathrm{i}2\pi\mathbf{q}\cdot\mathbf{r})$, introduced by the narrow gradient pulses and by the molecular dynamics expressed through the function, $P_s(\mathbf{r}|\mathbf{r}',t)$ which describes the conditional probability that a spin-bearing molecule at **r** migrates to $\mathbf{r}'$ after time t. The basic differential equation governing $P_s(\mathbf{r}|\mathbf{r}',t)$ is Ficks' law,

$$D_0\nabla'^2 P_s = \partial P_s/\partial t, \tag{1}$$

where D_0 is the molecular self-diffusion coefficient. P_s is subject to a boundary condition for the case of relaxing walls, namely

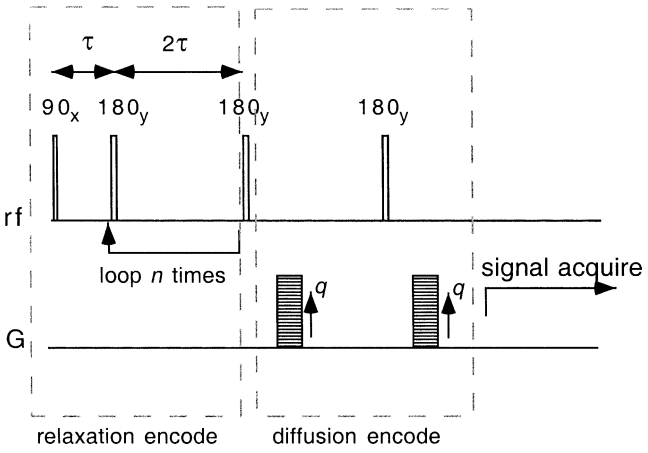

Fig. 1. NMR pulse sequence for two-dimensional encoding for relaxation and diffusion. The relaxation period is $t = 2n\tau$ for the preceding CPMG sequence.

$$D_0\hat{\mathbf{n}}\cdot\nabla' P_s + MP_s = 0, \tag{2}$$

where $\hat{\mathbf{n}}$ is the outward surface normal. Eqs. (1) and (2) may be tackled via the standard eigenmode expansion

$$P_s(\mathbf{r}|\mathbf{r}',t) = \sum_{n=0}^{\infty} \exp(-\lambda_n t) u_n(\mathbf{r}) u_n^*(\mathbf{r}'), \tag{3}$$

where the $u_n(\mathbf{r}')$ are an orthonormal set of solutions to the Helmholtz equation parameterized by the eigenvalue λ_n.

We choose here to investigate the case of the planar and spherical pore in the narrow gradient pulse approximation. The effect of finite width gradient pulses may be easily incorporated using the matrix method outlined in an earlier paper [26]. For the moment, and in the interests of simplicity, we seek to elucidate this simplest of all problems for two classical geometries. Eigenfunctions for the case of the planar and spherical boundaries have been given earlier [17].

The echo attenuation expression derived from the pulse sequence of Fig. 1 may be written

$$E_\Delta(\mathbf{q},t) = \int\int \rho(\mathbf{r},t) P_s(\mathbf{r}|\mathbf{r}',\Delta) \exp[\mathrm{i}2\pi\mathbf{q}\cdot(\mathbf{r}'-\mathbf{r})]\,\mathrm{d}\mathbf{r}\,\mathrm{d}\mathbf{r}', \tag{4}$$

where $\rho(\mathbf{r},t)$ reflects the spin relaxation taking place over the relaxation encoding time, t and is given by

$$\rho(\mathbf{r}',t) = \int \rho(\mathbf{r},0) P_s(\mathbf{r}|\mathbf{r}',t)\,\mathrm{d}\mathbf{r} \tag{5}$$

with $P_s(\mathbf{r}|\mathbf{r}',t)$ subject to Eq. (2). In general the two-dimensional experiment will allow for one $\mathbf{q}$ direction, which we shall define by spatial coordinate z, so that Eq. (4) is rewritten

$$E_\Delta(q,t) = \int\int \rho(z,t) P_s(z|z',\Delta) \exp[\mathrm{i}2\pi q\cdot(z'-z)]\,\mathrm{d}z\,\mathrm{d}z'. \tag{6}$$

Note that the PGSE encode time, Δ, is considered fixed. Of course, varying Δ and q while keeping t fixed or varying Δ and t while keeping q fixed leads to different, alternative, two-dimensional experiments. The expressions that we derive are general and allow for analysis of all three sets of experiments. For the planar pore case the gradient is applied along the z-direction normal to a pair of bounding planes and these relaxing planes are separated by a distance $2a$ and placed at $z = \pm a$. For the spherical case the gradient of magnitude q is applied along the polar axis of the spherical polar coordinate frame. The relaxing boundary is at a radial distance $r = a$ from the sphere center. The resulting expressions for $E_\Delta(q,t)$ are:

$$\begin{aligned}
E_\Delta(q,t) = {} & 2\sum_{k,n} \exp\left(-\frac{D_0\xi_k^2 t}{a^2}\right)\exp\left(-\frac{D_0\xi_n^2\Delta}{a^2}\right)\mathrm{sinc}(\xi_k)[1+\mathrm{sinc}(2\xi_k)]^{-1}[1 \\
& + \mathrm{sinc}(2\xi_n)]^{-1}\left\{\frac{2\pi qa\sin(2\pi qa)\cos(\xi_k+\xi_n)-(\xi_k+\xi_n)\cos(2\pi qa)\sin(\xi_k+\xi_n)}{[(2\pi qa)^2-(\xi_k+\xi_n)^2]}\right. \\
& \left. + \frac{2\pi qa\sin(2\pi qa)\cos(\xi_k-\xi_n)-(\xi_k-\xi_n)\cos(2\pi qa)\sin(\xi_k-\xi_n)}{[(2\pi qa)^2-(\xi_k-\xi_n)^2]}\right\}\frac{2\pi qa\sin(2\pi qa)\cos(\xi_n)-\xi_n\cos(2\pi qa)\sin(\xi_n)}{[(2\pi qa)^2-\xi_n^2]} \\
& + 2\sum_{k,m} \exp\left(-\frac{D_0\xi_k^2 t}{a^2}\right)\exp\left(-\frac{D_0\zeta_m^2\Delta}{a^2}\right)\mathrm{sinc}(\xi_k)[1-\mathrm{sinc}(2\xi_k)]^{-1}[1 \\
& + \mathrm{sinc}(2\zeta_m)]^{-1}\left\{\frac{2\pi qa\cos(2\pi qa)\sin(\xi_k+\zeta_m)-(\xi_k+\zeta_m)\sin(2\pi qa)\cos(\xi_k+\zeta_m)}{[(2\pi qa)^2-(\xi_k+\zeta_m)^2]}\right. \\
& \left. + \frac{2\pi qa\cos(2\pi qa)\sin(\zeta_m-\xi_k)-(\zeta_m-\xi_k)\sin(2\pi qa)\cos(\zeta_m-\xi_k)}{[(2\pi qa)^2-(\zeta_m-\xi_k)^2]}\right\}\frac{2\pi qa\cos(2\pi qa)\sin(\zeta_m)-\zeta_m\sin(2\pi qa)\cos(\zeta_m)}{[(2\pi qa)^2-\zeta_m^2]},
\end{aligned} \tag{7a}$$

Plane pore

where

$$\xi_{k,n}\tan\xi_{k,n} = Ma/D_0 \quad \text{and} \quad \zeta_m \cot\zeta_m = -Ma/D_0. \tag{7b}$$

Spherical pore

$$E_\Delta(q,t) = \sum_{l,n,k} a_l b_{nk} 16\pi^2(-1)^n a^3 \exp\left(-\frac{\alpha_{0l}^2 D_0 t}{a^2}\right) \times \exp\left(-\frac{\alpha_{nk}^2 D_0 \Delta}{a^2}\right)[(2\pi qa)^2 - (\alpha_{nk})^2]^{-1} \times [2\pi qa j_n(\alpha_{nk}) j_{n+1}(2\pi qa) - \alpha_{nk} j_n(2\pi qa) j_{n+1}(\alpha_{nk})] \times \int_0^a r\sin(\alpha_{0l}) j_n\left(\alpha_{nk}\frac{r}{a}\right) j_n(-2\pi qr)\,\mathrm{d}r, \tag{8a}$$

where

$$a_l = \frac{-3}{2\pi a^2}[j_0^2(\alpha_{0l}) - j_{-1}(\alpha_{0l}) j_1(\alpha_{0l})]^{-1} \times \left[\alpha_{0l}\cos(\alpha_{0l}) - \sin(\alpha_{0l})\alpha_{0l}^4\right], \tag{8b}$$

$$b_{nk} = \frac{2n+1}{2\pi a^3}[j_n^2(\alpha_{nk}) - j_{n-1}(\alpha_{nk}) j_{n+1}(\alpha_{nk})]^{-1}, \tag{8c}$$

and

$$\alpha_{nk}\frac{j_n'(\alpha_{nk})}{j_n(\alpha_{nk})} = -Ma/D_0. \tag{8d}$$

2.1. Diffusion–relaxation correlation

Of the three possible two-dimensional experiments, (q^2,t), (Δ,q^2), and (t,Δ), only the first clearly separates diffusion and relaxation effects and we shall limit our attention to this experiment alone. We first focus on the plane parallel pore of width $2a$. Inspection of Eqs. (7a) and (7b) shows that the effect of the relaxation encoding is especially simple. The relaxation is multi-exponential in time t, with relaxation time constants $a^2/D_0\xi_k^2$. The amplitudes of these modes are qa-dependent. Note that the ξ_k/a are the wave-numbers for the eigen-modes describing the heterogeneous relaxation of the fluid within the pore, and describe the spatial frequencies of these eigen-modes. Exactly as in Brownstein–Tarr theory, the slowest relaxation time corresponds to the principal (longest wavelength) mode where $k = 0$. For Ma/D_0 small, ξ_0 is $(Ma/D_0)^{1/2}$ and the dominant relaxation time is simply a/M. For Ma/D_0 large, ξ_0 is $\pi/2$ and the dominant relaxation time is $a^2/D_0(\pi/2)^2$. Note that ξ_0 falls in the range 0–$\pi/2$, ξ_1 in the range π–$3\pi/2$ and so on. Hence, the slowest (ξ_0) and next fastest (ξ_1) relaxation times are separated in magnitude by about a factor of 10.

By contrast the effect of diffusion encoding over the PGSE time Δ is a little more complex. Through the terms $\exp(-D_0\xi_n{}^2\Delta/a^2)$ and $\exp(-D_0\zeta_m{}^2\Delta/a^2)$ the PGSE dependence on q is governed by the roots ξ_n which fall in the range 0–$\pi/2$, π–$3\pi/2,\ldots$, as well as by the roots ζ_m which fall in the range $\pi/2$–π, $3\pi/2$–$2\pi,\ldots$ By contrast, only the roots ξ_k affect the relaxation which occurs in the CPMG time domain, t. In the PGSE encoding the $\xi_{k/a}$ and $\zeta_{m/a}$ play the role of wave-numbers for the eigen-modes describing the heterogeneous displacement of molecules within the pore.

Fig. 2 shows an example of a two-dimensional echo attenuation function, $E_\Delta(q,t)$ for the case $Ma/D_0 = 5.0$ and $D_0\Delta/a^2 = 0.2$, as slices in the qa planes. It is a feature of Brownstein–Tarr relaxation (i.e., the case $q = 0$) that the principal mode dominates the relaxation, so that multi-exponential character is seldom observed in practice, except at very large values of Ma/D_0. Even at infinite Ma/D_0 the amplitude of the principal (slowest relaxation) ξ_0 mode is nearly an order of magnitude greater than the amplitude of the secondary (next fastest) ξ_1 mode. One of the consequences of the combined PGSE-CPMG experiment is that the higher order relaxation modes are greater emphasized, an effect which is apparent in Fig. 2. As the parameter qa is increased the bi-exponential character of the T_2 relaxation becomes more obvious. Fig. 3 shows the relative amplitudes, A_1/A_0 of the ξ_1 and ξ_0 relaxation modes, as a function of qa. This figure demonstrates the utility of combined PGSE-relaxation encoding in more clearly revealing the higher order Brownstein–Tarr modes. Note that the asymptote of A_1/A_0 at large qa is independent of $D_0\Delta/a^2$ and is determined solely by Ma/D_0.

Our 2-D inverse Laplace analysis was performed with software developed by us and based on the method published by Ventkataramanan. In the case of the spherical pore it is around 10^{-10} of the smallest input value used. Machine errors were insignificant in determining transformation outcomes and the results shown

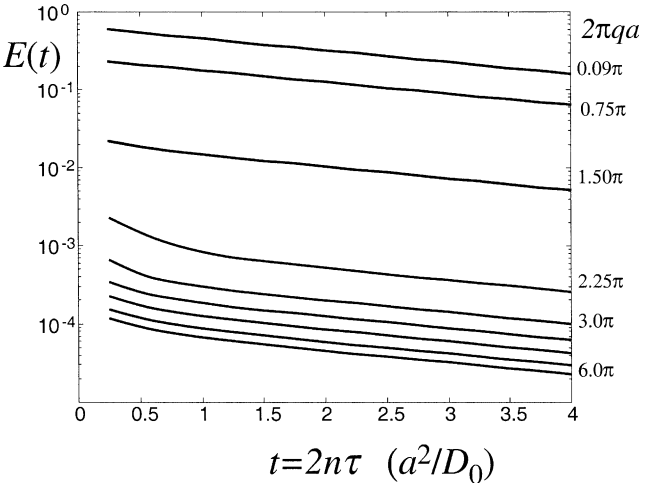

Fig. 2. Slices of two-dimensional echo attenuation function, $E_\Delta(q,t)$, at constant q. Increasing bi-exponential character is apparent as qa increases.

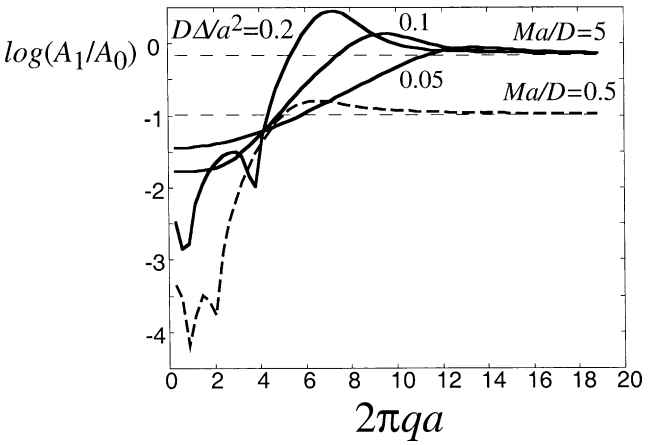

Fig. 3. Ratio of the secondary and primary modes for relaxation, as a function of $2\pi qa$ for two values of $Ma/D_0 = 5$ and $Ma/D_0 = 0.5$, for the case $D_0\Delta/a^2 = 0.2$. Note the enhancement for the secondary relaxation mode as qa increases.

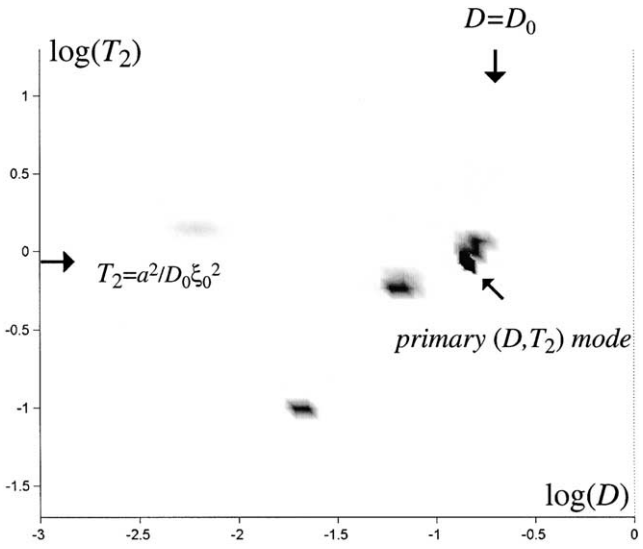

Fig. 4. Two-dimensional (D, T_2) map for the plane parallel pore, for the case $Ma/D_0 = 2$ and $D_0\Delta/a^2 = 0.2$. Dvalues are expressed in units of a^2/Δ and T_2 values in units of a^2/D_0. These maps were obtained by suppressing the amplitude of the primary relaxation–diffusion mode of by using a lower cutoff of $(qa)^2 = 0.15a^2/D_0\Delta$. The diagonal arrow indicates the position of the primary relaxation–diffusion mode obtained from the low-q data. The vertical arrow indicates D_0 while the horizontal arrow on the left indicates the position of the primary relaxation mode $T_2 = a^2/D_0\xi_k^2$.

here are robust under variations in eigenvalue truncation or stepsize effects. In carrying out a two-dimensional inverse Laplace analysis of the $E_\Delta(q,t)$ data, we have chosen to deliberately de-emphasize the principal diffusion–relaxation mode by using a lower $(qa)^2$ cutoff value of approximately $0.15a^2/(D_0\Delta)$ The choice of cutoff is not significant. It affects the relative amplitudes of the modes, but not their corresponding (D, T_2) coordinates in the 2-D plots that result from two-dimensional inverse Laplace transformation.

Fig. 4 shows an example of a (D, T_2) map for the plane parallel pore case, obtained for $Ma/D_0 = 2$ and $D_0\Delta/a^2 = 0.2$. This was calculated using a $401^2(q^2, t)$ input data set and a $50 \times 40(D, T_2)$ domain. In accordance with standard practice (*3*), regularisation was adjusted to minimize χ^2 with maximum smoothing. As a guide to Fig. 4, a number of arrows are used to indicate (D, T_2) reference features. The diagonal arrow indicates the position of the principal relaxation–diffusion feature which dominates as $qa > 0$. The principal (slow) relaxation mode, $T_2 = a^2/D_0\xi_0^2$ is shown with a horizontal arrow. Also shown, using a vertical arrow, is the free diffusion value, D_0.

Fig. 5 shows a set of (D, T_2) maps for the plane parallel pore case, for values of Ma/D ranging from 0.5 to 10 and for $D_0\Delta/a^2 = 0.1$, 0.2, and 0.3. The same data transformation conditions were used as for Fig. 4. Again the diagonal arrows indicate the position of the relaxation–diffusion feature which dominates as $qa > 0$ while the principal (slow) relaxation value, $T_2 = a^2/D_0\xi_0^2$ is shown with a horizontal arrow, and a vertical arrow, is used to indicate the free diffusion values, D_0. Also shown, using a horizontal arrow on the right hand side of the graph, is the high Ma/D_0 relaxation limit, $T_2 = a^2/D_0(\pi/2)^2$. These maps are remarkably rich in features and show a wide spread of diffusion and relaxation values, despite the simple geometry of the pore. Note that the restriction of $D_0\Delta/a^2$ to values less than 0.5 ensure that the curvature of the echo attenuation data in q^2-space remains consistent with apparent multi-exponential decay. We would emphasise that the choice of the maximum value of q^2 does not influence the position of the peaks found in the $D - T_2$ domain, but only their relative amplitude.

In interpreting these two-dimensional patterns, it is important to recognize that these are maps in which (D, T_2) features are separated in a wave-number domain, rather than in a spatial domain. The echo attenuation data arise from a superposition of modes. In converting the echo attenuation data to the Laplace domain these modes tend to become separated and identifiable. Note that the relaxation behavior at short t and the diffusion behavior at short Δ are complete mode sums, while the principal relaxation and diffusion modes, with eigen-value ξ_0, dominate in the long time limits.

In the (D, T_2) maps the following features are apparent:

(i) There exists a concentration of intensity in the region where the diffusion value takes its unrestricted value D_0, and the relaxation has the principal (slow) mode value $a^2/D_0\xi_0^2$. This feature moves to slower diffusion as $D_0\Delta/a^2$ increases, due to greater influence of wall collisions. This region also corresponds to the posi-

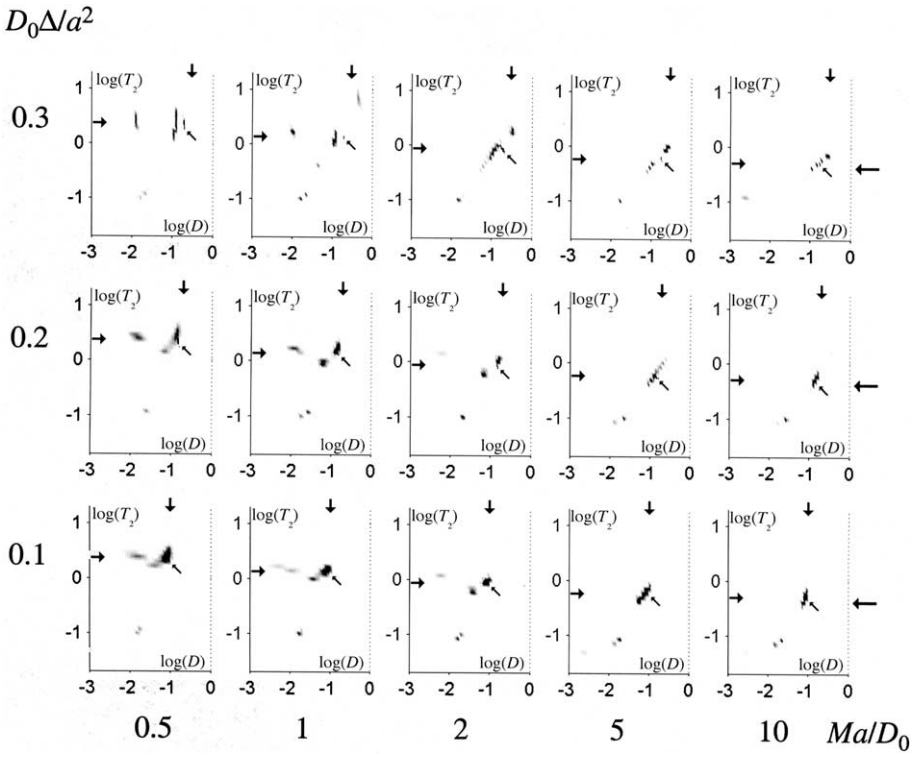

Fig. 5. Two-dimensional (D, T_2) maps for the plane parallel pore, as a function of Ma/D_0 and $D_0\Delta/a^2$. D values are expressed in units of a^2/Δ and T_2 values in units of a^2/D_0. These maps were obtained by suppressing the amplitude of the primary relaxation–diffusion mode of by using a lower cutoff of $(qa)^2 = 0.15a^2/D_0\Delta$. The diagonal arrow indicates the position of the primary relaxation–diffusion mode obtained from the low-q data. The vertical arrow indicates D_0 while the horizontal arrows on the left indicate the positions of the primary relaxation modes $T_2 = a^2/D_0\xi_k^2$. Horizontal arrows on the right indicate the Brownstein–Tarr limit for $Ma/D_0 \gg 1$, of $T_2 = a^2/D_0(\pi/2)^2$.

tion of the diagonal arrow which indicates the dominant (D, T_2) behavior.

(ii) There exists an isolated concentration of intensity at D and T_2 values about one order of magnitude slower than D_0 and faster than $a^2/D_0\xi_0^2$, respectively. This feature increases in intensity as Ma/D_0 increases.

(iii) There exists an isolated concentration of intensity at D about one order of magnitude slower than D_0 but with T_2 still at the slow mode value $a^2/D_0\xi_0^2$. This feature decreases in intensity as Ma/D_0 increases.

(iv) There exists a distinct diagonal grouping near the dominant $(D = D_0, T_2 = a^2/D_0\xi_0^2)$ position in which both D and T_2 values are strongly correlated. We note that the associated spread in T_2 values is smaller than the mode separation determined by the different ξ_k^2 values.

Feature (i) represents the dominant 2-D mode and corresponds to long wavelength, pore-averaged behavior for both the diffusion and relaxation domains. Feature (ii) represents a D and T_2 mode with common eigen-value ξ_1. This mode correspondence arises from the matching of the wave-vectors describing the initial coordinates of the propagator, P_s, with those of the spatial distribution of magnetization following the relaxation encoding. Since higher wave-number modes arise from short-range features, they tend to reflect the pore boundaries. The correlated (D, T_2) modes of feature (ii) arise from pore surface relaxation behavior as well as the diffusive perturbation associated with wall collisions. The strengthening of feature (ii) with increasing Ma/D_0 is consistent with the separability of the fluid into "wall" and "bulk" phases as Ma/D_0 becomes large. To that extent we may regard feature (ii) as being associated with fluid near the surface.

Feature (iii) by contrast arises from reduced diffusion but at the longest wavelength mode for relaxation. Here the geometric restriction to diffusion is uncoupled from the details of prior magnetisation distribution caused by relaxation at the wall. The strengthening of feature (iii) with decreasing Ma/D_0 is consistent with the indistinguishability of "wall" and "bulk" phases as Ma/D_0 becomes small. To that extend we may regard feature (iii) as being associated with "pore-averaged" behavior.

Feature (iv) is especially intriguing because the spread in relaxation times seen here lies between the Brownstein–Tarr modes, and is not predicted in a one-dimensional relaxation encoding experiment. To some extent this spread may arise from the ill-defined nature of the inverse Laplace transformation. However the strong correlation between diffusion and relaxation in feature

(iv) suggests that this diagonal spread is physical in origin. We attribute this effect to the subtle effects of relaxation over the diffusive encoding time, noting that the spread becomes more obvious as Ma/D_0 increases.

Fig. 5 compares the same plots obtained in the case of spherical pores of radius a. The features (i) to (iv) are again apparent, thus suggesting that the precise details of pore geometry are unimportant. In both the plane parallel pore and the spherical pore, one is able to identify separate (D, T_2) branches, one with diffusion and relaxation strongly correlated and one with a wide spread of D values weakly correlated with higher order relaxation modes.

Finally we note that the method described here applies also to (D, T_1) correlations in which the CPMG segment of the pulse sequence is replaced by an inversion recovery sequence. By means of T_1 encoding, wall relaxation effects can be examined without the complicating effects of dephasing caused by diamagnetic susceptibility inhomogeneity. The expressions derived in this work apply equally well to such analyses.

3. Conclusions

In their recent paper Hürlimann and Venkataramanan [20] show D-relaxation maps for a mixture of different molecular weight oils in which diffusion and relaxation are strongly correlated due to their respective dependence on molecular size. They also demonstrate that strong D-relaxation correlations exist in an interconnected porous medium with a wide distribution of pore sizes. These correlations arise from the respective dependence of apparent diffusion and relaxation on pore size. In the present paper we show that diffusion and relaxation for a single molecular species may be correlated within a pore of unique size, simply because of the eigen-mode structure of the solutions to the diffusion equations that govern both phenomena.

Note that the (D, T_2) analyses presented here are most relevant to the regime $D_0\Delta/a^2 \sim< 1$ and $Ma/D_0 >\sim 1$. In practical terms, and for small molecule (e.g. water) diffusion, this regime corresponds to pore dimensions several tens of microns or larger. In such systems the separability of diffusion and relaxation correlations for spins confined to simple pore shapes suggests the possibility of using (D, T_2) analysis to separate near-wall and bulk behavior. These two-dimensional plots, obtained by inverse Laplace transformation, may prove of value in discriminating surface and bulk fluid. We envisage particular applications to porous media and mesophase systems where boundary perturbations are of interest. The (D, T_2) correlations may also prove of interest in the study of biological cells, where cell wall transport plays an important role (see Fig. 6).

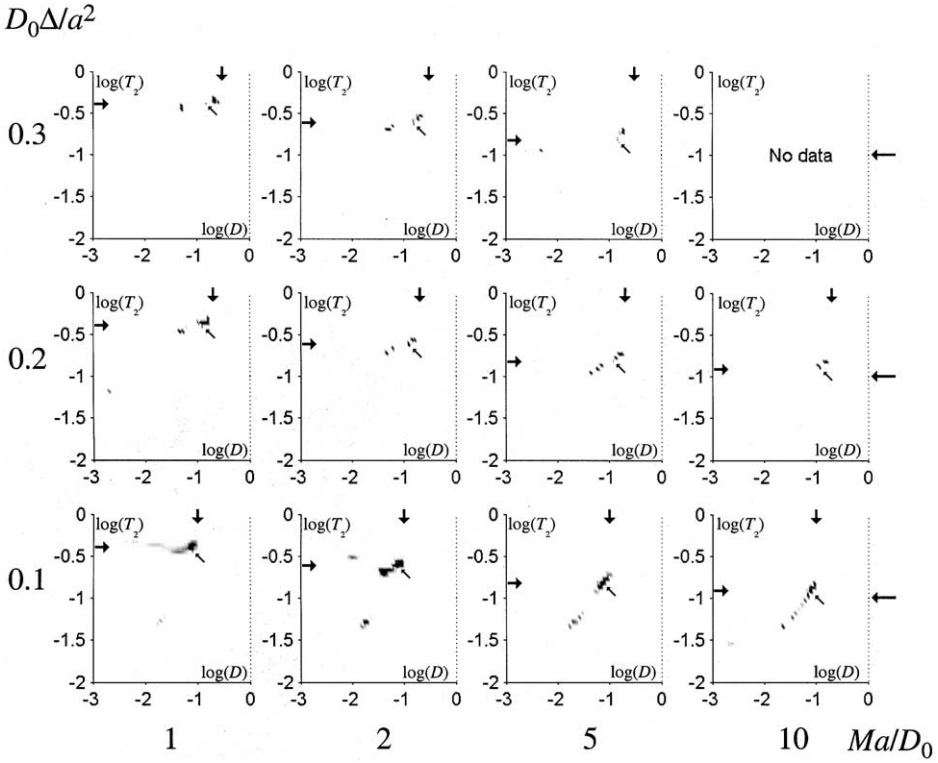

Fig. 6. As for Fig. 6 but for spherical pores. The vertical arrow indicates D_0 while the horizontal arrows on the left indicate the positions of the primary relaxation modes $T_2 = a^2/D_0\xi_k^2$. Horizontal arrows on the right indicate the Brownstein–Tarr limit for $Ma/D_0 \gg 1$, of $T_2 = a^2/D_0(\pi)^2$.

Acknowledgments

The authors are grateful to the New Zealand Foundation for Research, Science and Technology, and the Royal Society of New Zealand Marsden Fund, and Centres of Research Excellence Fund, for Grant Support. During the course of preparing this paper we have become aware that Hürlimann et al. have also been calculating relaxation–diffusion effects in simple pores and will soon submit an article to another journal. We are grateful to Dr Hürlimann for advising us of this.

References

[1] K.R. Brownstein, C.E. Tarr, Importance of classical diffusion in NMR studies of water in biological cells, Phys. Rev. A 19 (1979) 2446.
[2] C.L. Lawson, R.J. Hanson, Solving Least Squares Problems, Prentice-Hall, Englewood Cliffs, NJ, 1974.
[3] S.W. Provencher, Comput. Phys. Commun. 27 (1982) 229.
[4] K.P. Whittall, A.L. Mackay, Quantitative interpretation of NMR relaxation data, J. Magn. Reson. 84 (1989) 134–152.
[5] D.W. McCall, D.C. Douglass, E.W. Anderson, Self-diffusion by means of nuclear magnetic resonance spin echo techniques, Ber. Busenges. Phys. Chem. 67 (1963) 336–340.
[6] E.O. Stejskal, J.E. Tanner, Spin-diffusion measurements: spin echoes in the presence of a time-dependent field gradient, J. Chem. Phys. 42 (1965) 288–292.
[7] J.E. Tanner, E.O. Stejskal, Restricted diffusion of protons in colloidal systems by the pulsed gradient spin echo method, J. Chem. Phys. 49 (1968) 1768–1777.
[8] P.T. Callaghan, Pulsed field gradient nuclear magnetic resonance as a probe of liquid state molecular organization, Austr. J. Phys. 37 (1984) 359–387.
[9] P. Stilbs, Fourier transform pulsed gradient spin echo studies of molecular diffusion, Progr. Nucl. Magn. Reson. Spectrosc. 19 (1987) 1–45.
[10] P.T. Callaghan, Principles of Nuclear Magnetic Resonance Microscopy, OUP, Oxford and New York, 1991.
[11] D.G. Cory, A.N. Garroway, Measurement of translational displacement probabilities by NMT: an indicator of compartmentation, Magn. Reson. Med. 14 (1990) 435–444.
[12] P.T. Callaghan, D. McGowan, F. Zelaya, K.J. Packer, Influence of field gradient strength in NMR studies of diffusion in porous media, Magn. Reson. Imaging 9 (1991) 663–671.
[13] P.T. Callaghan, A. Coy, D. Macgowan, K.J. Packer, F.O. Zelaya, Diffraction-like effects in NMR diffusion studies of fluids in porous solids, Nature 351 (1991) 467–469.
[14] P.P. Mitra, P.N. Sen, L.M. Schwartz, P. Le Doussal, Diffusion propagator as a probe of the structure of porous media, Phys. Rev. Lett. 68 (1992) 3555–3558.
[15] P.T. Callaghan, A. Coy, T.P.J. Halpin, D. Macgowan, K.J. Packer, F.O. Zelaya, Diffusion in porous systems and the influence of pore morphology in pulsed gradient spin echo nuclear magnetic resonance studies, J. Chem. Phys. 97 (1992) 651–662.
[16] A. Coy, P.T. Callaghan, Pulsed Gradient Spin Echo nuclear magnetic resonance for molecules diffusing between partially reflecting rectangular barriers, J. Chem. Phys. 101 (1994) 4599–4609.
[17] P.T. Callaghan, Pulsed gradient spin echo NMR for planar, cylindrical and spherical pores under conditions of wall relaxation, J. Magn. Reson. A 113 (1995) 53–59.
[18] M.M. Britton, R.G. Graham, K.J. Packer, Magn. Reson. Imaging 19 (2001) 325.
[19] J.H. Lee, C. Labadie, C.S. Springer, Two-dimensional inverse laplace transformation NMR-altered relaxation times allow detection of exchange-correlation, J. Am. Chem. Soc. 115 (1993) 7761–7764.
[20] M.D. Hürlimann, L. Venkataramanan, Quantitative measurement of two-dimensional distribution functions of diffusion and relaxation in grossly inhomogeneous fields, J. Magn. Reson. 157 (2002) 31–42.
[21] L. Venkataramanan, Y.Q. Song, M.D. Hürlimann, Solving Fredholm intergrals of the first kind with tensor product structure in 2 and 2.5 dimensions, IEEE Trans. Signal Process. 50 (2002) 1017–1026.
[22] Y.Q. Song, L. Venkataramanan, M.D. Hürlimann, M. Flaum, P. Frulla, C. Straley, T_1-T_2 correlation spectra obtained using a fast two-dimensional Laplace inversion, J. Magn. Reson. 154 (2002) 261–268.
[23] L.Z. Xiao, Y.R. Du, C.H. Ye, Observation of the relaxivity and thickness of surface phase in the porous rock with combination of PFG NMR and relaxation measurement, Sci. China Ser. A 39 (1996) 974–980.
[24] W.F.J. Slijkermann, J.P. Hofman, Determination of surface relaxivity from NMR diffusion measurement, Magn. Reson. Imaging 16 (1998) 541–547.
[25] D. van Dusschoten, P.A. de Jager, H. van As, Extracting diffusion constants from echo-time-dependent PFG NMR data using relaxation time information, J. Magn. Reson. A 116 (1995) 22–28.
[26] P.T. Callaghan, A simple matrix formalism for the spin echo analysis of restricted diffusion under generalised gradient waveforms, J. Magn. Reson. 129 (1997) 74–84.